Communications in Physics, Vol. 33, No. 3 (2023), pp. 297-308
DOI: https://doi.org/10.15625/0868-3166/18152

Asymmetric tunneling of holes through a semiconductor junction in an arbitrary magnetization configuration

Cao Tien Khoa, **Dinh Thuy Van**, **Dang Thi Huong**, **Phan Dinh Quang and Do Thi Hue**†

Thai Nguyen University of Education,
No. 20, Luong Ngoc Quyen Street, Quang Trung ward, Thai Nguyen city, Vietnam

E-mail: †huedt@tnue.edu.vn

Received 8 March 2023
Accepted for publication 15 May 2023
Published 10 August 2023

Abstract. Spilanthes acmella L. Murr *is a medicinal herb with many valuable biological activities such as clearing heat, detoxifying, dissipating phlegm, antiseptic, pain relief, antifungal, anti-inflammatory... In this work, we used Spilanthes acmella L. Murr extract to synthesize silver nanoparticles (L.AgNPs) to combine and enhance the activity of silver and Spilanthes acmella L. Murr extract in antibacterial and antifungal activities. The reaction parameters were investigated to find the most optimal conditions for synthesizing L.AgNPs, such as $AgNO_3$ volume, solution pH, and reaction temperature. UV-VIS absorption spectra were used to analyze the influence of the reaction parameters. The functional groups on the L.AgNPs as well as the Spilanthes acmella L. Murr extract were found by infrared absorption (FTIR) spectroscopy. The crystal structure of the synthesized L.AgNPs was determined by X-ray diffraction (XRD) spectroscopy. On the basis of the synthesized L.AgNPs, the antifungal activity was investigated on the strains: A. flavus (Af), A. brasiliensis (Ab), C. Albicans (Ca), and antibacterial: Staphylococcus aureus (SA), Pseudomonas aeruginosa (PA) was performed to compare the activity of the antibiotic Ampicilline 100 mg/mL.*

Keywords: L.AgNPs; Spilanthes acmella L. Murr; biosynthesis; antibacterial; antifungal.
Classification numbers: 81.05.Gc; 87.19.xg.

1. Introduction

The symptoms of pain and inflammation are both a protective response of the body against pathogens and a pathological response that can damage tissues and cause many unpleasant symptoms for the patient [1]. The use of pharmaceutical drugs to relieve pain and inflammation often

causes many side effects, so using herbal medicinal herbs to treat diseases is a trend of interest to scientists [2]. Spilanthes acmella L. Murr is a precious medicinal herb, the scientific name is Spilanthes oleracea L, belonging to the daisy family (Asteraceae) [3]. Plants and chrysanthemums contain essential oil compounds spilanthol; eudesman solid, sterol and a nonreducing polysaccharide [3-4]. Spilanthes acmella L. Murr has the taste of numbing the tongue, warming, clearing heat, detoxifying, dissipating phlegm and antiseptic, relieving pain. Leaves can be used as vegetables, plants and flowers are often used in oriental medicine to treat diseases such as headache, fever, sore throat, intermittent malaria, bronchitis, asthma, whooping cough, tuberculosis, toothache, tooth decay, rheumatism, bone pain, paralysis, boils, wounds, venomous snake bites, itchy sores, swollen hematomas... [5-6]. With many valuable biological activities, Spilanthes acmella L. Murr is a plant with great potential for pharmacology in the future.

AgNPs are one of the most interesting types of nanomaterials because, in addition to the properties of metal nanomaterials in general, such as photocatalysis [7], electrical properties [8], magnetic properties [9], and photoelectric ability [10], they also have outstanding antibacterial and bactericidal properties [11]. Because of these specific physicochemical properties, AgNPs have many applications in different fields, such as detection and decomposition of toxic organic pigments [12-14], biosensors [15], drug delivery and biomolecules [16], important materials in electro-optical devices [17], antimicrobial, antiviral, and antifungal ... [18-20]. There are many different methods for the synthesis of AgNPs such as chemical reduction [21-23], electrochemical methods [24-25], photochemical methods [26-27], radiation methods [28-29], and biological methods [30-31] ... The general principle of these methods is to use $AgNO_3$ as the initial precursor, using reducing agents to reduce Ag^+ ions to Ag^0 atoms. These atoms clump together in specific ways in the presence of surfactants to form colloidal L. AgNPs in solution. However, to synthesize bio-friendly L. AgNPs, the synthesis method from plant extracts is the most optimal solution. In the extracts of some plant species, there are groups of substances that act as biological reducing agents to reduce Ag^+ ions such as green tea, mint, guava leaves, and linden root... they have been used as raw materials for synthesis of L. AgNPs by green method [32-34].

From studying the active ingredients and properties of Spilanthes acmella L. Murr, We synthesized L. AgNPs from Spilanthes acmella L. Murr extract in order to combine the medicinal properties of Spilanthes acmella L. Murr with anti-bacterial and anti-viral properties of L. AgNPs to create a material with better activity. In this paper, in addition to investigating the factors affecting the synthesis of L. AgNPs to find the optimal parameters for the reaction, studies on the antibacterial and antifungal properties of the synthetic materials are studied.

2. Experiment

2.1. Synthesis of L. AgNPs using Spilanthes acmella L. Murr leaf extract

Prepare the Spilanthes acmella L. Murr extract

The extract of Spilanthes acmella L. Murr was made according to the diagram shown in Fig. 1. Fresh Spilanthes acmella L. Murr was collected in Phu Binh district, Thai Nguyen province, Vietnam including part of the stem, leaves, and flowers. The plants were washed several times with water to remove dirt. After being dried at 50˚C to kill yeast, the plants were ground into a dry powder by an agate mortar to form a relatively fine powder. 2g powder was dissolved in 20 ml of water and distilled at 100˚C for 1 h. The solution was then centrifuged at 5000 rpm for 15 min

to remove large particles. To obtain the final extract, the solution after centrifugation was filtered through a 0.2 µm filter and stored at 4˚C.

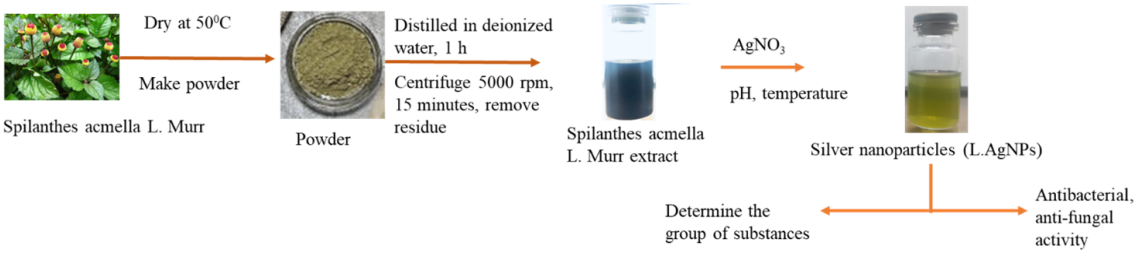

Fig. 1. Synthesis diagram of L. AgNPs using *Spilanthes acmella L. Murr* leaf extract.

Investigate the influence of factors on the growth of L. AgNPs

To optimize the synthesis of L. AgNPs, the factors affecting the formation and growth of L. AgNPs were investigated in detail. Three series of experiments were conducted with the change of one of three factors: $AgNO_3$ concentration, pH and reaction temperature.

i) The first experiment was performed with a change in $AgNO_3$ concentration: 4 ml of the extract was adjusted to pH = 8 by adding 1M HCl or 1M NaOH, then divided into 4 equal parts into 4 flasks 20 ml capacity. Add 2 mM $AgNO_3$ to the 4 reaction flasks in 7.5 ml, 10 ml, 12 ml and 15 ml volumes respectively, while stirring at 800 rpm, 40˚C. After about 10 min of reaction, the solution changed from the dark green color of the extract to a light green, sleightly cloudy color. The reaction was maintained for 2 hours.

ii) The second experiment was performed with a change of 6 pH values: 5.09; 6.06; 7.11; 8.11; 9.16 and 10.13 by adjusting the amount of 1M HCl and 1M NaOH added to the solution containing 1 ml of extract. Add 15 ml of 2 mM $AgNO_3$ to each reaction flask. The solution was also stirred at 800 rpm, 40˚C for about 2 hours.

iii) The third experiment was performed by varying the reaction temperature: 20˚C, 40˚C, 60˚C and 80˚C while the flasks all had 1 ml of extract, 15 ml of 2 mM $AgNO_3$ and pH = 8.

2.2. Study on the activity of L. AgNPs

Antifungal activity

The solution containing L.AgNPs was dispersed in DMSO solvent into the ratios of 100 mg/ml, 50 mg/ml, 25 mg/ml. The antifungal activity of L.AgNPswas carried out by diffusion method in the plate [8]. The fungal strains used for testing are A. flavus (Af), A. brasiliensis (Ab), C. Albicans (Ca) grown on PDA agar. The solution of L. AgNPs with the above concentrations was dripped into the jelly wells. Petri dishes were grown at 30˚C in an incubator for 3 days and the antifungal diameter was measured. The control used in this experiment was the antibiotic Ampicilline 100 mg/mL.

Antibacterial activity test

The selected bacteria strains are all strains that cause dangerous infections for humans and animals. *Staphylococcus aureus* (SA) is a species of facultative aerobic Gram-positive staphylococcus and is the most common cause of bacterial infections among staphylococci. Coagulase-positive *SA* is one of the most common and dangerous human pathogens, because of its toxicity and antibiotic resistance [35]. *Pseudomonas aeruginosa* (PA) can cause urinary tract infections, lower respiratory tract infections, meningitis, endocarditis, otitis media, etc. In particular, sepsis is an infection with a very high mortality rate [36]. *Citrobacter freundii* (CF) is an anaerobic bacteria. It belongs to the Enterobacteriaceae family and is known to cause a number of opportunistic infections, as well as many respiratory, urinary, and blood infections [37]. The antibacterial activity test method was carried out in the same way as the antifungal activity test method.

Measurement methods

The morphology and size of the L. AgNPs were observed through SEM images obtained on the system Hitachi S4800 scanning electron microscope (SEM) operating at 10 kV. The optical properties of L. AgNPs were studied on absorption spectroscopy using a Jasco V-770 UV–Vis spectrophotometer in the range of 250 nm – 1000 nm. The crystal structure of L. AgNPs obtained from X-ray diffraction spectroscopy using an X-ray diffractometer (Bruker D8 Advance, Germany) operated at 30 kV with Cu-Ka radiation (wavelength of $\lambda = 0.154056$ nm) with parallel-beam geometry between 300 to 800 range system. The Fourier transform infrared (FTIR) spectroscopy on the system Cary 600 Series FTIR spectrometer, range 7500 - 2800 cm^{-1} shown the functional groups in the extract and on the L. AgNPs. The anti-inflammatory activity of the material was determined through the cell inhibition rate based on optical density measurement using an Infinite F50 instrument (Tecan, Männedorf, Switzerland).

3. Results and discussion

Morphology and structure of L. AgNPs

The obtained L. AgNPs using $AgNO_3$ and the Spilanthes acmella L. Murr leaf extract have a pseudospherical shape and are well dispersed in solution. The average size of L. AgNPs was determined by Image software ranging from 45 nm ± 10 nm. Compared with the synthesis of L. AgNPs by chemical reduction method, the L. AgNPs synthesized from plant extracts in general and Spilanthes acmella L. Murr extracts, in particular, have a wider size distribution. However, the obtained L. AgNPs are better uniform shape and size than the results of previous reports [38-40]. The morphology and size of the L. AgNPs are shown by SEM images on two different scales of 100 nm and 50 nm (Fig. 2). In general, the particles are relatively uniform in size, about 45 nm. However, there are still particles as large as 100 nm and some as small as about 10 nm. This is unavoidable when the particles synthesized by reducing agents are compounds present in the plant extracts. The reaction time is much longer than that of chemical-reducing agents. Therefore, the development of L. AgNPs mainly focuses on the last stage in Lamer's kinetic scheme [41]. During this stage, small particles can clump together to form larger particles depending on their distance in solution to form large particles. At the same time, because the reduction rate is slow, there are still seeds generated, they combine with the L. AgNPs available in the solution to create

large-sized particles or combine to form small L. AgNPs. The L. AgNPs produced later are much smaller in size than the previously synthesized ones.

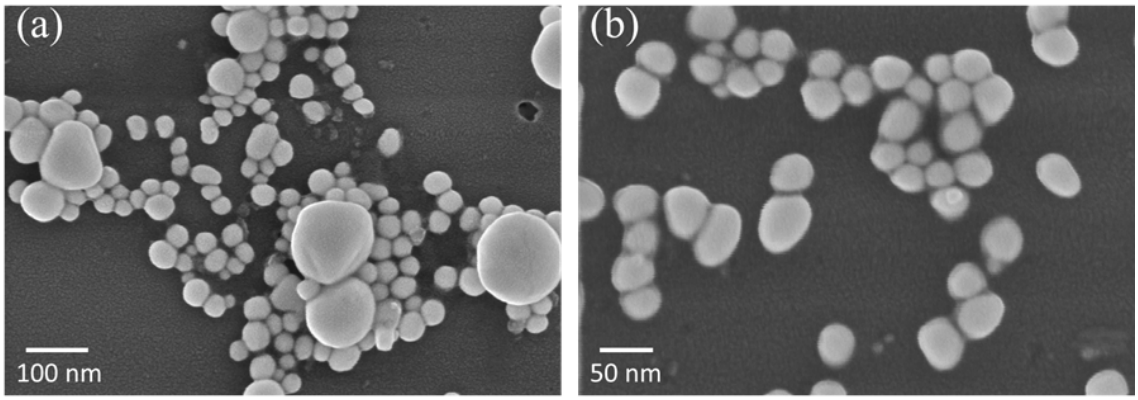

Fig. 2. SEM image of *L. AgNPs* using $Ag(NO_3)$ and *Spilanthes acmella L. Murr* leaf extract with two scales of 100 nm (a) and 50 nm (b).

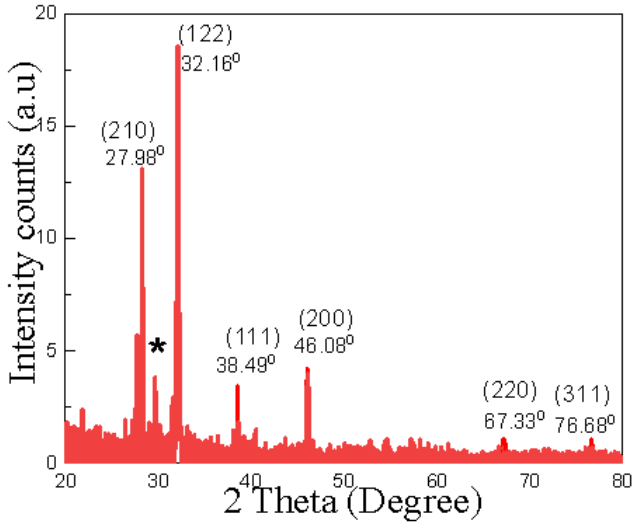

Fig. 3. XRD spectrum of L. AgNPs using $AgNO_3$ and *Spilanthes acmella L. Murr* leaf extract.

The crystal structure of obtained L. AgNPs was investigated through XRD diffraction (Fig. 3). The positions of diffraction peaks characteristic for silver phases are determined at 2θ angles: 27.98˚, 32.16˚, 38.49˚, 46.08˚, 67.33˚ and 76.68˚ respectively with lattice planes (210), (122), (111), (200), (220) and (311) [JCPDS file No. 04-0783]. This shows that the synthesized L. AgNPs have an fcc-type crystal structure like the natural crystal structure of Ag. There is also a diffraction peak marked with an asterisk (*) at position 29.75˚ representing the diffraction phase of AgO [JCPDS file no. 84-1108].

Figure 4 is the infrared absorption spectrum (FTIR) of Spilanthes acmella L. Murr extract, and obtained L. AgNPs. The FTIR spectrum provides information on the bond groups involved in the synthesis of L. AgNPs. The red line is the FTIR spectrum of Spilanthes acmella L. Murr extract with the position of the peaks representing the vibrations of the groups of substances. For example, the infrared absorption peak at 3385.98 cm^{-1} corresponds to strong stretching vibrations of hydroxyl and amino groups of alcohols and phenolic substances. This peak shifts to 3664 cm^{-1} on the FTIR spectrum of L. AgNPs. This suggests that there is an association of organic groups with Ag^{+} through free amine groups or carboxyl groups. The infrared absorption peak at position 2927.97 cm^{-1} is attributed to the binding of CH to the benzene ring. Peak position at 1633.46 cm^{-1} corresponds to the C − −O of the amide I protein stretching mode. The functional groups detected the FTIR spectrum in the Spilanthes acmella L. Murr extract are present in the groups of natural substances such as flavonoids, saponins, steroids- terpenoids and tannins... The presence of these groups shows the resistance ability antibacterial, anti-fungal, anti-inflammatory of the Spilanthes acmella L. Murr extract. The antibacterial and antifungal properties of L. AgNPs have also been confirmed in many reports [18-20]. Therefore, the synthesis of L. AgNPs by Spilanthes acmella L. Murr extract can combine activity and provide better applications.

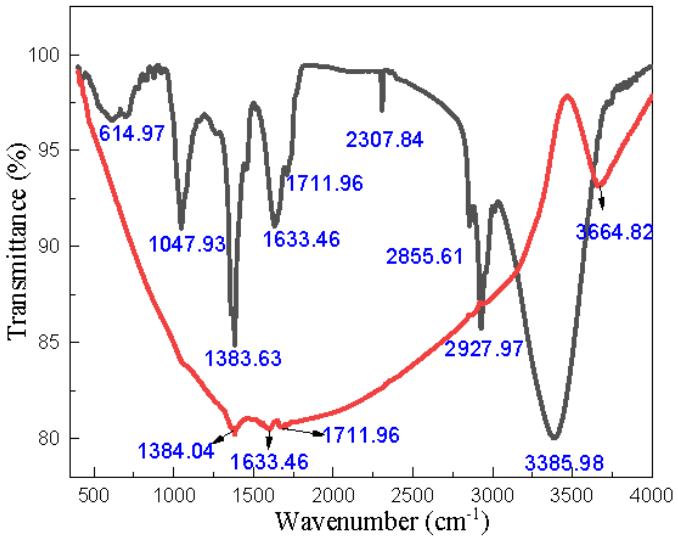

Fig. 4. (Color online) FTIR spectra of *Spilanthes acmella L. Murr* extract (black line) and L. AgNPs (red line).

The influence of factors on the growth of L. AgNPs

Figure 5 is the absorption spectra and normalized absorption spectra of L. gNPs solutions obtained by changing one of three factors: $AgNO_3$ concentration (a, b), solution pH (c, d) and reaction temperature (e, f). When the reaction temperature and pH of the solution were kept constant, the volume of $AgNO_3$ in the reaction flasks was adjusted to increase from 7.5 ml, 10 ml, 12.5 ml and 15 ml. It can be seen that the absorption spectra of the solutions are similar, with the maximum resonance peak at 670 nm. According to TEM images, the average size of L. AgNPs

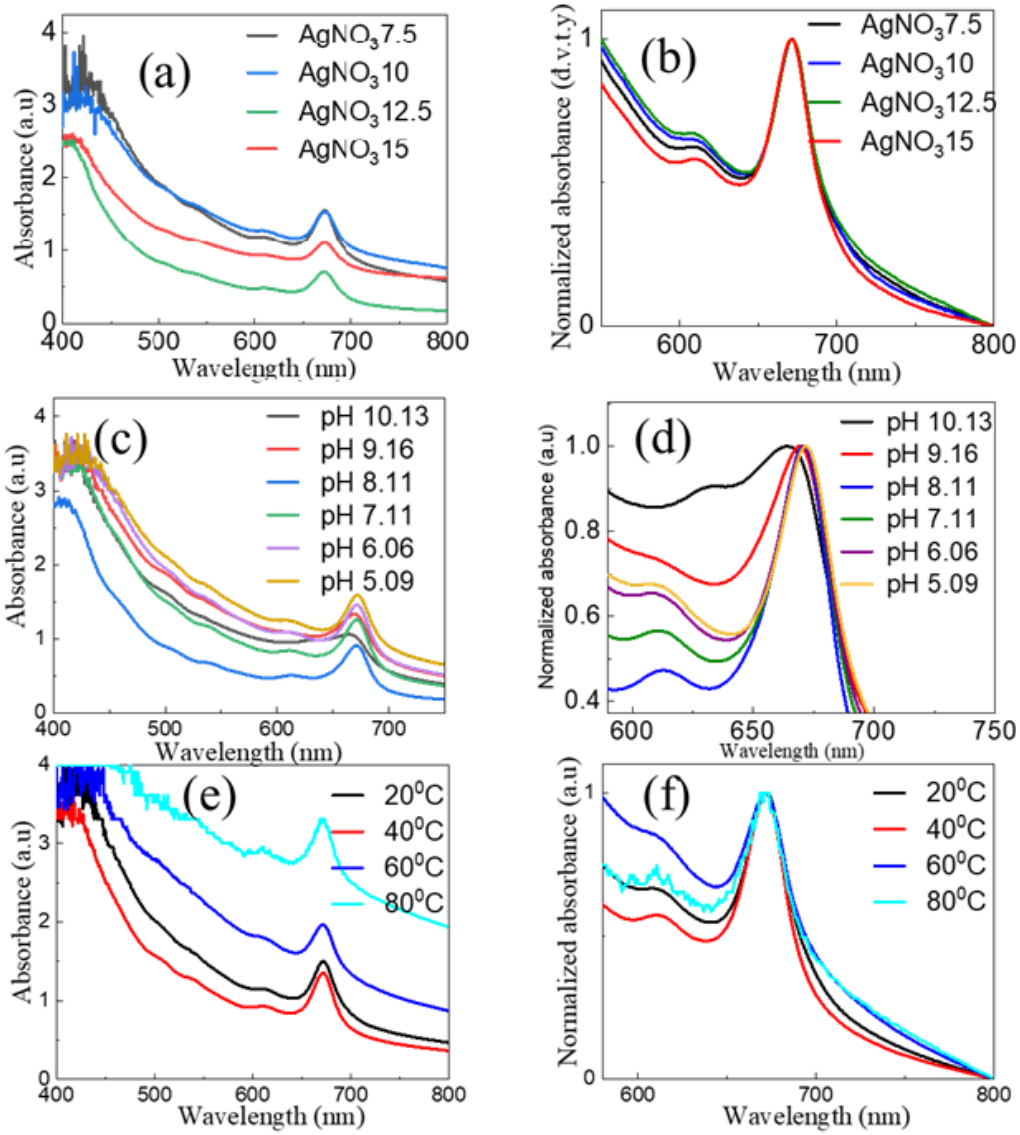

Fig. 5. Absorption spectra and normalized absorption spectra of L. AgNPs solutions when changing the volume of $AgNO_3$ (a, b), changing pH (c, d) and changing the reaction temperature (e, f).

is about 45 nm. These AgNPs will strongly absorb light at 400 nm - 500 nm if they are dispersed in water (refractive index 1.33). However, the refractive index of the medium surrounding the obtained L. AgNPs is higher than that of water (approximately 2), so the plasmon resonance peak shifts towards the long wave. This is the optical properties of metal nanoparticles in general and AgNPs in particular. The absorption intensity decreased from 1.55 to 0.68 when the volume of $AgNO_3$ decreased from 7.5 ml to 12.5 ml but increased to 1.09 when the volume of $AgNO_3$

increased to 15 ml. At the same time, the high absorbance of the solutions in the 400 nm range indicates that the extraction volume used in the experiments is redundant. The use of the residual extract to create a surface-stable environment for L. AgNPs. The normalized absorption spectra (Fig. 5b) show that the half-width of the absorption spectrum when using 15 ml of $AgNO_3$ is the smallest, indicating that the synthesized particles are more uniform. Therefore, we selected the volume of $AgNO_3$ 15 ml/1 ml of extract to conduct the next experiments.

To find the appropriate pH for the granulation reaction, small volumes of 1 M HCl and 1 M NaOH were added to the solution so that the pH of the pre-reaction solution took on 5.09; 6.06; 7.11; 8.11; 9.16 and 10.13, respectively. It can be seen with the same volume of $AgNO_3$ but the consumption of extract when solution pH = 8.11 is the most. At the same time, the normalized absorption spectra also show that the half-spectral width of the solution when pH = 8.11 is the narrowest, showing that the particles are most uniform in shape and size. This assertion is completely consistent with Lamer's kinetic mechanism when explaining the growth of metal nanoparticles in solution. The faster the reaction rate, the better the similarity of the resulting particles.

The same analysis applies to the absorption and normalized absorption spectra (Figure 5e,f) of the solutions synthesized at different temperatures: 20˚C, 40˚C, 60˚C, and 80˚C, a reaction temperature of 40˚C can be seen for the best quality L. AgNPs. Thus, through survey experiments, we have found the most optimal conditions for synthesizing L. AgNPs as follows: 1ml of extract, 15ml of 2mM $AgNO_3$, pH = 8.11, reaction temperature 40˚C, stirring reaction at 800 rpm for about 2 hours.

Applications of L. AgNPs

Antifungal results of L. AgNPs are shown in Table 1, Fig. 6 and Fig. 7. In all experiments, solvent DMSO was used as the negative control and the antibiotic Ampicilline 100 mg/mL was used as the positive control. The results showed that using DMSO no sterility ring was observed while using the antibiotic and all investigated concentrations of the L. AgNPs showed antifungal activity. This ability is as good as the current antibiotic Ampicilline. However, depending on the concentration of the L. AgNPs, the level of resistance is different, specifically: at a concentration of 100 mg/mL, it has the highest ability to inhibit all three fungal strains. Among them, resistance to CA strain is the best.

Table 1. Antifungal zone diameter using L. AgNPs with different concentrations, negative control (DMSO) and positive control (Ampicilline)

	Antifungal zone diameter (mm)				
Fungal strains	**Ampicilin100 mg/mL (+) control**	**DMSO (+) control**	**100 mg/mL (G1)**	**75 mg/mL (G2)**	**50 mg/mL (G3)**
AF	14.0	0	14.66	11.0	9.0
CA	10.0	0	16.66	13.33	9.67
AB	12.33	0	13.66	11.66	8.0

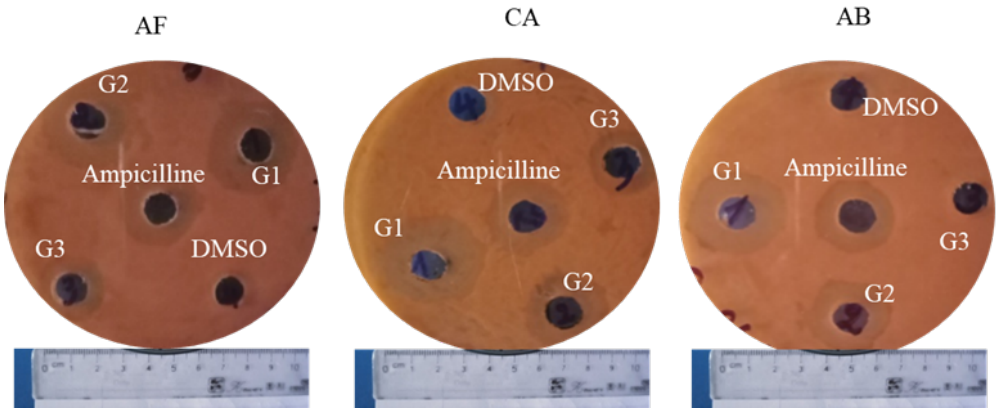

Fig. 6. Antifungal results of L. AgNPs with different concentrations (G1, G2, G3), negative control (DMSO) and positive control (Ampicilline).

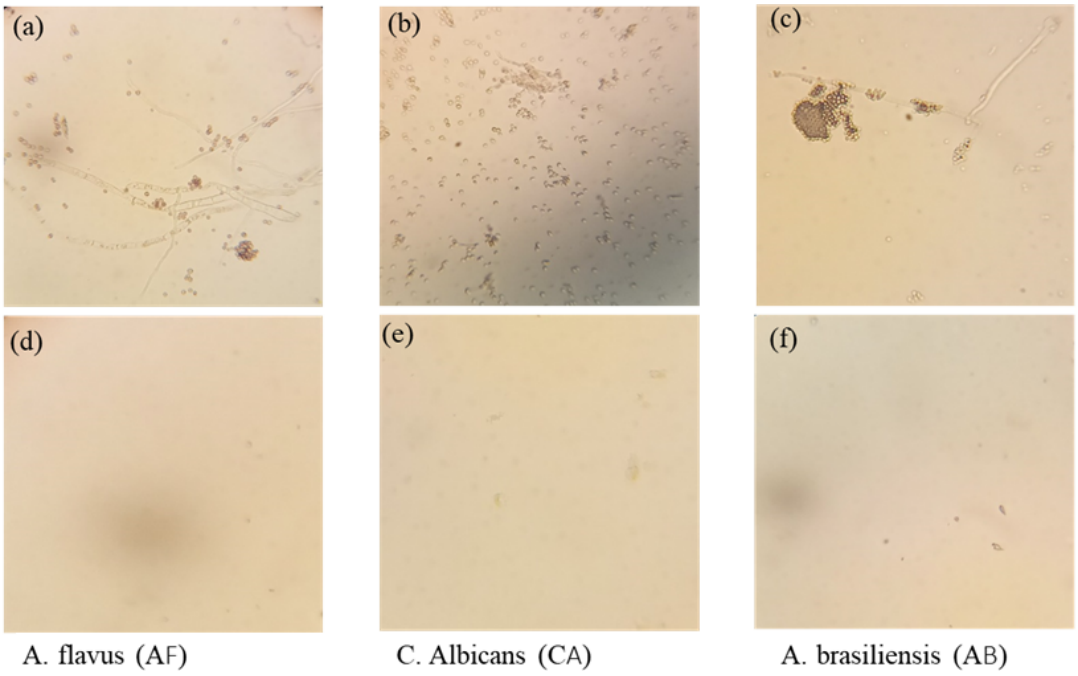

Fig. 7. Microscopic image of mycelium and spores in the absence of L. AgNPs (a, b, c) and in the presence of L.AgNPs (d, e, f).

When observed under the microscope, different fungal strains have different shapes of mycelium and spores. In the absence of L. AgNPs, the image of mycelium and fungal spores can be clearly seen. In the region where L. AgNPs were present, they damaged the cell membrane and inhibited the formation of mycelium (Fig. 7). Therefore, the mycelium and spores were not observed under the microscope in samples with the presence of L. AgNPs.

Figure 8 shows that L. AgNPs have very good antibacterial activity against all 3 tested strains of bacteria equivalent to currently used antibiotics, the best resistance concentration is 100 mg/mL. The most strongly inhibited bacteria the *Staphylococcus aureus* strain. This result is better than the antibacterial result of AgNPs synthesized by chemical methods [18-20].

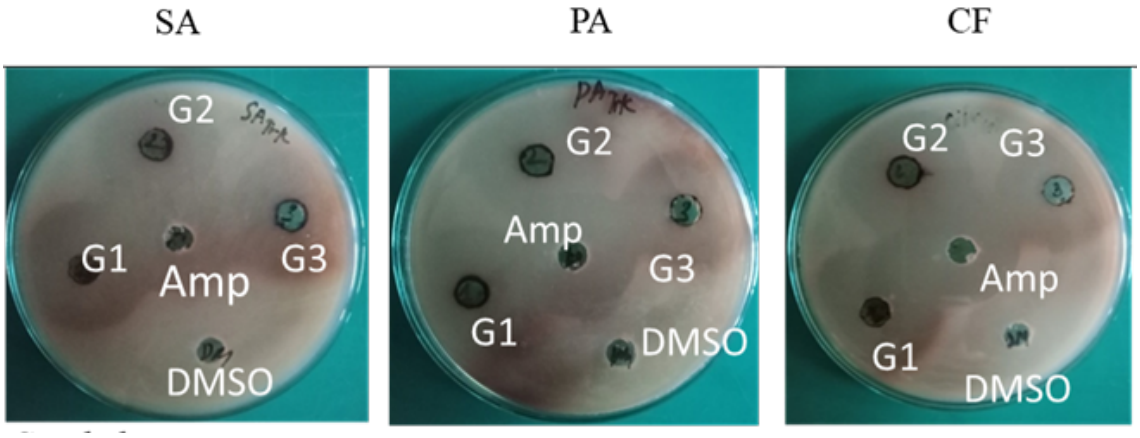

Fig. 8. Antibacterial results of L. AgNPs with different concentrations (G1, G2, G3), negative control (DMSO) and positive control (Ampicilline).

4. Conclusions

In the present study, we report the bioreduction of silver ions into AgNPs using Spilanthes acmella L. Murr leaf extract, which acts as both a reducing and capping agent for L. AgNPs. The synthesized L. AgNPs have an average size of about 45 nm ± 10 nm. The peaks of the plasmon resonance of the L. AgNPs solutions are at 670 nm. The XRD diffraction spectrum shows that the synthesized L. AgNPs have an fcc crystal structure similar to the natural crystal structure of Ag. FTIR analysis demonstrated that flavonoids, saponins, steroids- terpenoids and tannins play a major role in this bioreduction process and increases the antibacterial and antifungal activities of L. AgNPs. Investigating the influence of factors on the formation and development of L. AgNPs, we found that the optimal parameters for the synthesis of L. AgNPs are 15 ml of 2 mM $AgNO_3$/1ml extract 0.1g/ml, pH = 8, stirring at 800 rpm, at 40˚C for 2 h. These compounds are all compounds with high antibacterial and antifungal activities. This has been confirmed based on the results when using synthetic L. AgNPs against fungal strains such as *A. flavus* (AF), *A. brasiliensis* (AB), *C. Albicans* (CA), and bacteria strains such as *Staphylococcus aureus* (SA), *Pseudomonas aeruginosa* (PA), *Citrobacter freundii* (CF). The results show that the antifungal and antibacterial activities of L. AgNPs are even better than those of ampicillin antibiotics. The ability to fight fungi and bacteria is the best with the concentration of L. AgNPs 100 mg/ml.

Acknowledgments

The present research was supported by a grant from TNUE code CS.2023.07.

References

[1] V. S. Dandin, P. M. Naik, H. N. Murthy, S. Y. Park, E. J. Lee and K. Y. Paek, *Rapid regeneration and analysis of genetic fidelity and scopoletin contents of micropropagated plants of Spilanthes oleracea L*, J. Hortic. Sci. Biotechnol. **89** (2014) 79.

[2] N. Chaachouay, A. Douira and L. Zidane, *Herbal medicine used in the treatment of human diseases in the Rif, Northern Morocco*, Arab J. Sci. Eng. **47** (2022) 131.

[3] E. Spinozzi, M. Ferrati, C. Baldassarri, L. Cappellacci, M. Marmugi, A.Caselli, G. Benelli, F. Maggi, A. Petrelli, *A review of the chemistry and biological activities of Acmella oleracea ("jambù", Asteraceae), with a view to the development of bioinsecticides and acaricides*, Plants **11** (2022) 2721.

[4] R. Abdul Rahim, P.A. Jayusman, N. Muhammad, N. Mohamed, V. Lim, N. H. Ahmad *et al.*, *Potential Antioxidant and Anti-Inflammatory Effects of Spilanthes acmella and Its Health Beneficial Effects: A Review.* Int. J. Environ. Res. Public Health. **18** (2021) 3532.

[5] V. Prachayasittikul, S. Prachayasittikul, S. Ruchirawat, V. Prachayasittikul. *High therapeutic potential of Spilanthes acmella: A review*, EXCLI J. **12** (2013) 291.

[6] S. Dubey, S. Maity, M. Singh, S.A Saraf and S. Saha, *Phytochemistry, Pharmacology and Toxicology ofSpilanthes acmella: A Review*, Adv. Pharmacol. Sci. **2013** (2013) 423750.

[7] W. L. Silva, D. M. Druzian, L. R. Oviedo, P. C. L. Muraro and R. V. Oviedo, *L. AgNPs for photocatalysis and biomedical applications* in *Silver micro-nanoparticles - properties*, IntechOpen, 2021.

[8] S. Moharana, A. Subhrasmita Gadtya, R. Nayak and R. Naresh Mahaling, *Synthesis, dielectric and electrical properties of silver-polymer nanocomposites* in *Silver Micro-Nanoparticles*, IntechOpen, 2021.

[9] A. Michałowska and A. Kudelski, *The first silver-based plasmonic nanomaterial for shell-isolated nanoparticle-enhanced Raman spectroscopy with magnetic properties*, Molecules **27** (2022) 3081.

[10] B. Lv, Y. Liu and W. Wu, *Local large temperature difference and ultra-wideband photothermoelectric response of the silver nanostructure film/carbon nanotube film heterostructure*, Nat. Commun. **13** (2022) 1835.

[11] C. Luna, E.D. Barriga-Castro, A. Gómez-Treviño, N.O Núñez and R. Mendoza-Reséndez, *Microstructural, spectroscopic, and antibacterial properties of silver-based hybrid nanostructures biosynthesized using extracts of coriander leaves and seeds*, Int. J. Nanomed. **11** (2016) 4787.

[12] J. Singh and R. K. Soni, *Efficient charge separation in Ag nanoparticles functionalized ZnO nanoflakes/CuO nanoflowers hybrids for improved photocatalytic and SERS activity*, Colloids Surf. A Physicochem. Eng. Asp. **626** (2021) 127005.

[13] R. A. Abo-Elmagd, R. A. Hamouda and M.H. Hussein, *Phycotoxicity and catalytic reduction activity of green synthesized Oscillatoria gelatin-capped L.AgNPs*, Sci. Rep. **12** (2022) 20378.

[14] N. Khandannasab, Z. Sabouri, S. Ghazal and M. Darroudi, *Green-based synthesis of mixed-phase L.AgNPs as an effective photocatalyst and investigation of their antibacterial properties*, J. Mol. Struct. (2019) 127411.

[15] P. P. Austin Suthanthiraraj and A. K. Sen, *Localized surface plasmon resonance (LSPR) biosensor based on thermally annealed silver nanostructures with on-chip blood-plasma separation for the detection of dengue non-structural protein NS1 antigen*, Biosens. Bioelectron. **132** (2019) 38.

[16] P. Prasher, M. Sharma, H. Mudila, G. Gupta, A. K. Sharma, D. Kumar, K. Dua, *Emerging trends in clinical implications of bio-conjugated L.AgNPs in drug delivery*, Colloid Interface Sci. Commun. **35** (2020) 100244.

[17] X. Yan, Y. Zhou, W. Liu, S. Liu, X. Hu, W. Zhao and D. Yuan, *Effects of silver nanoparticle doping on the electro-optical properties of polymer stabilized liquid crystal devices*, Liq. Cryst. **47** (2020) 1131.

[18] M. Hasanin, M. A. Elbahnasawy, A. M. Shehabeldine, *Ecofriendly preparation of Silver nanoparticles-based nanocomposite stabilized by polysaccharides with antibacterial, antifungal and antiviral activities*, Biometals **34** (2021) 1313.

[19] A. Naganthran, G. Verasoundarapandian, F. E. Khalid, M. J. Masarudin, A. Zulkharnain, N.M. Nawawi *et al.*, *Synthesis, characterization and biomedical application of L.AgNPs*, Materials **15** (2022) 427.

[20] M. A. Sayed, T. M. A. A El-Rahman and H.K. Abdelsalam, *Attractive study of the antimicrobial, antiviral, and cytotoxic activity of novel synthesized silver chromite nanocomposites*, BMC Chem. **16 (2022)** 39.

[21] M. Gakiya-Teruya, L. Palomino-Marcelo and J. C. F. Rodriguez-Reyes, *Synthesis of highly concentrated suspensions of silver nanoparticles by two versions of the chemical reduction method*, Methods Protoc. **2** (2019) 3.

[22] A. Ścigała, R. Szczęsny, P. Kamedulski, M. Trzcinski and E. Szłyk, *Copper nitride/silver nanostructures synthesized via wet chemical reduction method for the oxygen reduction reaction*, J. Nanopart. Res. **25** (2023) 23.
[23] C. Gangwar, B. Yaseen, I. Kumar, N. K. Singh and R. M. Naik, *Growth kinetic study of tannic acid mediated monodispersed L.AgNPs synthesized by chemical reduction method and its characterization*, ACS Omega, **6** (2021) 22344.
[24] K. Nešović and V. Mišković-Stanković, *A comprehensive review of the polymer-based hydrogels with electrochemically synthesized Silver nanoparticles for wound dressing applications*, Polym. Eng. Sci. **60** (2020) 1393.
[25] S. M. Yang, H. K. Yen, K.C Lu, *Synthesis and Characterization of Indium Tin Oxide Nanowires with surface modification of L.AgNPs by electrochemical method*, Nanomater. **12** (2022) 897.
[26] N. Jara, N.S Milán, A. Rahman, L. Mouheb, D. C. Boffito, C. Jeffryes, S.A. Dahoumane, *Photochemical synthesis of gold and silver nanoparticles—A review*, Molecules **26** (2021) 4585.
[27] A. A.Yaqoob, K. Umar and M. N.M. Ibrahim, *Silver nanoparticles: various methods of synthesis, size affecting factors and their potential applications–a review*, Appl. Nanosci. **10** (2020) 1369.
[28] M. Bekhit, M. N. Abu el -naga, R. Sokary, R. A. Fahim, N. M. El-Sawy, *Radiation-induced synthesis of tween 80 stabilized Silver nanoparticles for antibacterial applications*, J. Environ. Sci. Health A **55** (2020) 1210.
[29] L. Freitas de Freitas, G. H. C. Varca, J.G. Dos Santos Batista, A. Benévolo Lugão, *An overview of the synthesis of gold nanoparticles using radiation technologies*, Nanomater. **8**(2018) 939.
[30] E. Sreelekha, B. George, A. Shyam, *A comparative study on the synthesis, characterization, and antioxidant activity of green and chemically synthesized silver nanoparticles*, BioNanoSci. **11** (2021) 489.
[31] R. Kotcherlakota, S. Das and C. R. Patra, *Chapter 16 - Therapeutic applications of green-synthesized silver nanoparticles* in *Green synthesis, characterization and applications of nanoparticles*, Elsevier, 2019, pp. 389–428.
[32] W. Zhang and W. Jiang, *Antioxidant and antibacterial chitosan film with tea polyphenols-mediated green synthesis silver nanoparticle via a novel one-pot method*, Int. J. Biol. Macromol. **155** (2020) 1252.
[33] M. Ovais, A. T. Khalil, A. Raza, M. A. Khan, I. Ahmad, N. U. Islam, Z. K. Shinwari, *Green synthesis of Silver nanoparticles via plant extracts: beginning a new era in cancer theranostics*, Nanomedicine **11**(2016) 3157.
[34] K. Govindaraju, K. Krishnamoorthy, S. A. Alsagaby, G. Singaravelu, & M. Premanathan, *Green synthesis of Silver nanoparticles for selective toxicity towards cancer cells*, IET Nanobiotechnol. **9** (2015) 325.
[35] A. H. Azam and Y. Tanji, *Peculiarities of staphylococcus aureus phages and their possible application in phage therapy*, Appl. Microbiol. Biotechnol. **103** (2019) 4279.
[36] T. Evans*, Diagnosis and management of sepsis*, Clin Med (Lond). **18** (2018) 146.
[37] L. H. Liu, N. Y. Wang, A. Y. J. Wu, C. C. Lin, C. M. Lee and C. P. Liu, *Citrobacter freundii bacteremia: Risk factors of mortality and prevalence of resistance genes*, J. Microbiol. Immunol. Infect. **51** (2018) 565.
[38] K. Ranoszek-Soliwoda, E. Tomaszewska, K. Małek, G. Celichowski, P. Orlowski, M. Krzyzowska *et al.*, *The synthesis of monodisperse silver nanoparticles with plant extracts*, Colloids Surf. B: Biointerfaces **177** (2019) 19.
[39] S. S. Dakshayani, M. B. Marulasiddeshwara, M. N. S. Kumar, G. Ramesh, P. R. Kumar, S. Devaraja and R. Hosamani, *Antimicrobial, anticoagulant and antiplatelet activities of green synthesized L.AgNPs using Selaginella (Sanjeevini) plant extract*, Int. J. Biol. Macromol. **135** (2019) 787.
[40] S. Ahmed, M. Saifullah, M. Ahmad, B. L. Swami and S. Ikram, *Green synthesis of silver nanoparticles using Azadirachta indica aqueous leaf extract*, J. Radiat. Res. Appl. Sci. **9** (2016) 1.
[41] J. Lin, Z. Yang, X. Zhao, H. Ji, C. Peng, B. Sui *et al.*, *Kinetics and mechanistic insights into the hydrothermal synthesis of alumina microrods*, Chem. Eng. Sci. **244** (2021) 116817.